Journal of NUCLEAR SCIENCE and TECHNOLOGY, Supplement 1, p. 248–252 (March 2000)

Dose Rate Analyses around the Equatorial and Divertor Ports during ITER In-Vessel Components Maintenance

S. Mori[*,†], A. Ito[**], S. Sato[**], K. Ako[**], E. Tada[**], K. Shibanuma[**], Y. Hattori[***] and H. Iida[***]

[*1] *Kawasaki Heavy Industries, Ltd.*
[*2] *Japan Atomic Energy Research Institute*
[*3] *ITER Joint Central Team*

The shutdown dose rates around the equatorial and divertor maintenance ports of ITER were evaluated with the 2-D/3-D combined approach, using the three-dimensional continuous-energy Monte Carlo code, MCNP-4B and the two-dimensional discrete ordinate code, DOT3.5. The neutron flux-to-shutdown dose rate conversion factor is derived with the two-dimensional geometry using the THIDA code system and the assumed operation scenario, i.e. the neutron fluence of 0.3 MWa/m^2 in ten years of operation. The dose rate around the equatorial and divertor ports after 10^6 seconds (11.6 days) after reactor shutdown ranges from 100 to 200 μ Sv/h. Attempts to further reduce the dose rate by improving the shield design were made to follow the principle of ALARA.

KEYWORDS: Fusion reactor, Tokamak, ITER, Maintenance, Shield, Dose rate, Vacuum vessel ports, Neutron Stream ing,Divertor, Monte Carlo method, Discrete ordinate method, Induced activity

I. Introduction

The dose rate in the cryostat of the International Thermonuclear Experimental Reactor (1) (ITER) during the maintenance of in-vessel components must be low enough (100 μSv/h as the design target) to make hands-on maintenance by personnel possible. As shown in **Fig. 1**, twenty large size ports for various purposes, 1 to 2 meter wide X2 to 3 meter high, are connected to the vacuum vessel in the top, middle (equatorial), and lower regions, respectively. The top ports are used for cooling pipe routing, the equatorial ports for blanket maintenance and plasma heating, and the lower ports for divertor maintenance and vacuum pumping. Personnel access points are between the primary closure plates of these ports and the cryostat. The dose rate after shutdown is enhanced by neutron streaming effect through these large size ports as well as through small size gaps and slits (below several centimeters) between adjacent blanket modules and between port shield plugs and port walls. It is required that neutron flux transmitted through these ports and the spatial distribution of induced activities by those neutrons be evaluated correctly. A series of calculations, i.e. neutron transport calculation during reactor operation – decay gamma-ray source distribution due to induced activities – gamma-ray transport calculation after reactor shutdown must be conducted systematically. As far as we know, however, no systematic code system for three-dimensional dose rate calculation has been established worldwide. In this study the neutron flux around the equatorial and lower divertor ports were evaluated using the 2-D/3-D combined approach, i.e. the two-dimensional discrete ordinates method and the three-dimensional Monte Carlo method.

In the next chapter the calculation method are described, and the calculation results for the equatorial maintenance port and the lower divertor ports both for maintenance and pumping are presented in Chapter III.

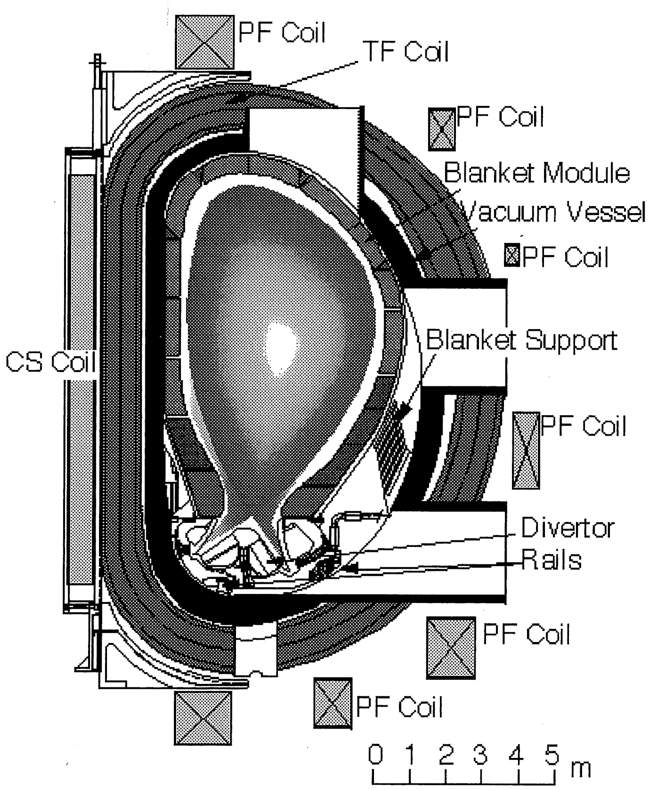

Fig. 1 Vertical cross section of the ITER in-vessel components

[*1] *6-5,2-chome Minamisuna, Koto-ku, Tokyo 136-8588*
[*2] *Tokai-mura, Naka-gun, Ibaraki 319-1195*
[*3] Max-Planck-Institut fuer Plasma Physik, *Boltzmannstrasse 2, 85748 Garching bei, Muenchen Germany*
† Corresponding author, Tel. +81-3-3615-5147, Fax. +81-3-3640-9497, E-mai: mori_s@khi.co.jp

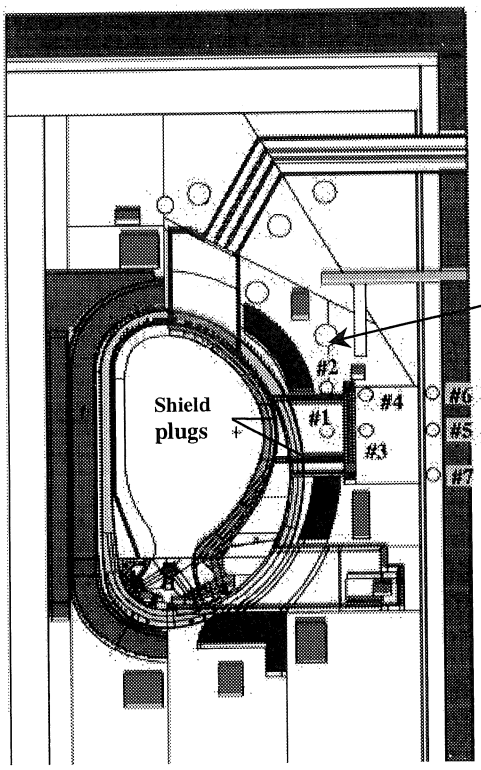

Fig. 2 Vertical cross section of the 3-D geometrical model of ITER for MCNP-4B (# indicates the ID number of track length estimators)

II. Calculation method

1. 2-D/3-D Combined Approach

In the ITER shielding design, the three-dimensional continuous-energy Monte Carlo code, MCNP-4B(2) is used as a standard tool. The two-dimensional discrete ordinate method such as DOT3.5 (3) is also used for the purpose of the preliminary study on shielding structure, e.g. to reduce radiation streaming effects. The JENDL-3 based cross section libraries (4)(5) are used in these calculations. For the shielding design analyses, a systematic calculation of the shutdown dose rate is required. It must include the following calculations: (1) neutron flux distribution in space and energy during reactor operation, (2) spatial and energy distribution of decay gamma-ray source intensity after reactor shutdown, (3) decay gamma-ray flux distribution in space and energy. Here, the 2-D/3-D combined approach is adopted. The decay gamma-ray source distribution is calculated with the THIDA code system (6) using the 2-D neutron flux distribution obtained with DOT3.5. The decay gamma-ray flux and the biological dose rate are calculated with DOT3.5 using the gamma-ray source distribution.

The neutron flux-to-shutdown dose rate conversion factor is defined as the ratio of shutdown dose rate to the operational neutron flux in the unit of [μSv/h]/[$cm^{-2}s^{-1}$]. Induced activity calculation is performed based on the assumed ITER operation scenario, i.e. the neutron fluence of 0.3 MWa/m^2 in ten years of operation and on the cooling time of 10^6 seconds (11.6 days) after shutdown. In the previous paper (7) it was found that the neutron flux can be represented by the fast neutron flux (E>0.1 MeV) in this approach. By multiplying the fast neutron flux evaluated by the three-dimensional calculation by the conversion factor, the shutdown dose rate is obtained in the three-dimensional configuration of MCNP-4B.

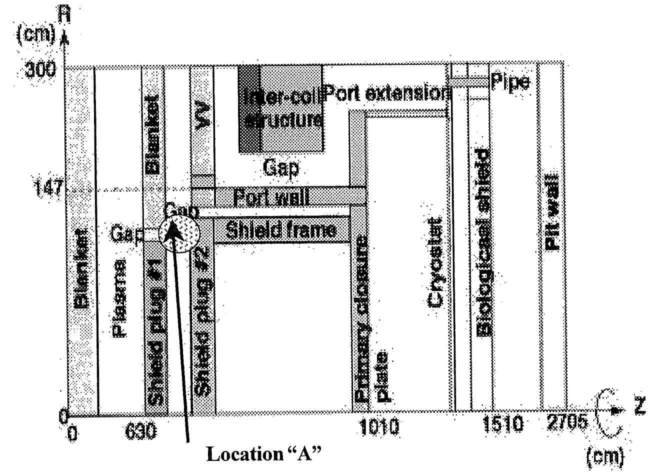

Fig. 3 2-D RZ model for the equatorial maintenance port for the in duced activity analysis by THIDA-2 (Dimensions are for the initial configuration.)

2. Calculation Models

The vertical cross section of the MCNP-4B geometrical model is shown in **Fig. 2**. This model includes all of the main tokamak components such as the blanket modules, the vacuum vessel, the divertor cassettes, the top ports, the equatorial ports, the divertor ports, the superconducting magnets, the cryostat, and the biological shield. The divertor pumping port is included in this model. In the case of the divertor maintenance port, there is no cryo-pump in the port. The model is a 1/40 torus sector model (9^o) of ITER. D-T fusion neutrons are generated in the plasma according to the plasma density distribution with 1.5 GW fusion power. The fast neutron flux was evaluated with the volumetric track length estimators. The weight window technique, space-energy dependent splitting and Russian Roulette variance reduction procedure, were used to reduce the variance of the calculated neutron flux.

The two-dimensional RZ model of DOT3.5 for the equatorial maintenance port is illustrated in **Fig. 3**, which is a local simplified model of the port. The port with the rectangular cross section is modeled as a circular cylinder. The 42 group neutron and 21 group gamma-ray cross section library, FUSION-40(5) was used with P5 expansion. Angular quadrature of space is a 166 forward biased set.

This model was used for the parametric study of the shield configuration such as the gap width and the shield plug thickness. The decay gamma-ray transport calculation was performed with the distributed gamma-ray source generated by the ACT4 code in the THIDA-2 code system, using the same geometrical model and the 54 group gamma-ray cross sec-

Table 1 Material composition and their dimensions for the initial and final configurations

Components	Material volume fraction	Thickness (cm)
Blanket	SS316:70%, Water:30%	58
Shield plug #1	SS316:70%, Water:30%	58
Gap b/w blanket and plug #1	Void	4 (5)*
Vacuum vessel	SS316:60%, water:40%	64
Equatorial port wall	SS316:60%, water:40%	20
Shield plug 2	SS316:60%, water:40%	64
Gap b/w port wall and plug #2	Void	2 (4)*
Primary closure plate	SS316:60%, water:40%	28 (40)*
Inter-coil structure (Front part)	SS316:100%	
Inter-coil structure (Rear part)	SS316:20%	
Cryostat	SS316:100%	5
Biological shield	Concrete:100%	126
Pit wall	Concrete:100%	200

* Values in parentheses are for the final configuration.

tion library, GROUPIN[6].

The material composition and the main dimensions of the model (e.g. gap width and shield plug thickness) are shown in **Table 1**. The "initial configuration" is based on the initial shield design and the "final configuration" is based on the improved shield design both from the shielding and structural points of view. The atomic number densities of the steel are shown in **Table 2**, which are based on the element composition of SS316LN-IG[8], the main structural and shielding material.

III. Calculation Results

1. Two-Dimensional Calculation

The fast neutron flux contour obtained with DOT3.5 for the final configuration is shown in **Fig. 4**. The fast neutron flux behind the primary closure plate is about 4 to 8×10^6 cm^{-2}s^{-1}. The dose rate contour around the closure plate 10^6 s after shutdown is shown in **Fig. 5**. The dose rate behind the primary closure plate is about 60 to 120μSv/h. Main contributors to the dose rate are ^{54}Mn, ^{58}Co and ^{60}Co produced from the iron and nickel components and the cobalt impurity in the stainless steel, SS316LN-IG. The conversion factor in the space between the primary closure plate and the cryostat is about 1.5×10^{-5} [μSv/h]/[cm^{-2}s^{-1}].

The fast neutron flux and the dose rate behind the primary closure plate for the initial configuration are about 8 to 10×10^6 cm^{-2}s^{-1} and 160 to 200mSv/h,, which are larger than those of the final configuration. The conversion factor is about 2×10^{-5} [μSv/h]/[cm^{-2}s^{-1}].

The main causes of the difference between the initial and final configurations are the gap widths and the thickness of

Table 2 Atomic number densities of SS316LN-IG used in the induced activity analysis

(Unit in 10^{24} atoms/cm^3)

Element	Number density	Element	Number density
^{10}B	1.74916E-06	Fe	5.56000E-02
^{11}B	7.08600E-06	Co	4.05200E-05
C	8.94700E-05	Ni	9.96800E-03
N	2.38700E-04	Cu	7.51600E-05
O	5.97100E-06	Zr	1.04700E-06
Al	8.85100E-05	Nb	2.57030E-06
Si	8.50300E-04	Mo	1.24500E-03
^{31}P	3.85500E-05	Sn	8.04700E-07
S	1.11726E-05	Ta	2.64000E-07
K	6.10800E-07	W	2.59280E-07
Ti	1.49600E-04	Pb	1.81542E-07
V	3.75000E-06	Bi	1.82800E-07
Cr	1.60700E-02	TOTAL	8.52250E-02
Mn	1.56500E-03		

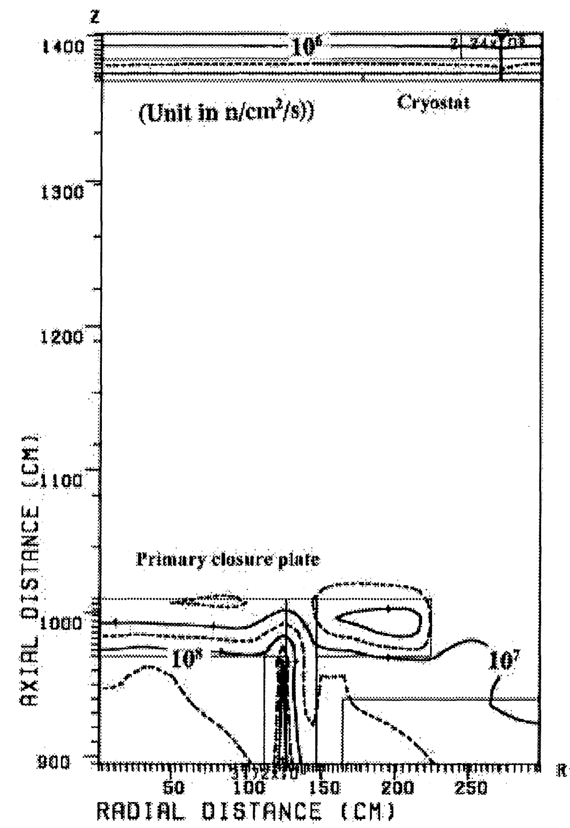

Fig. 4 Fast neutron flux contour for the final configuration obtained with DOT3.5 for the final configuration of the equatorial maintenance port

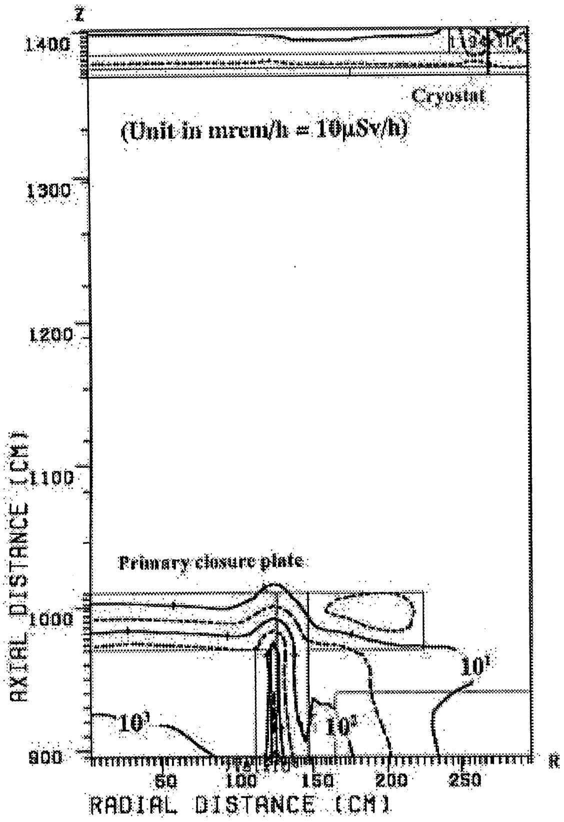

Fig. 5 Decay gamma-ray dose rate contour for the final configuration 10^6 seconds after shutdown for the equatorial maintenance port

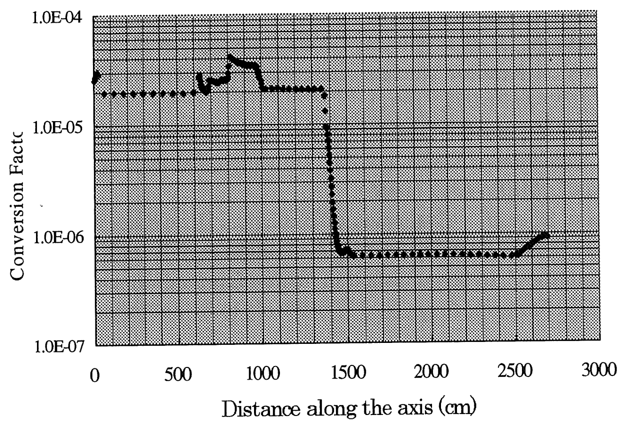

Fig. 6 Spatial distribution of the flux-to-dose conversion factor for the initial configuration along the port center axis (Z) in the unit of (μSv/h)/(n/cm2/s) for the cooling time of 10^6 seconds

the primary closure plate as shown in Table 1. The conversion factors for the two configurations are also different by about 25%.

The neutron streaming could be further reduced by a factor of five if a shield block is placed behind the gap (Location "A" in Fig.3), though the feasibility of such a design is not yet investigated.

Axial distribution (in the Z direction) of the flux-to-dose

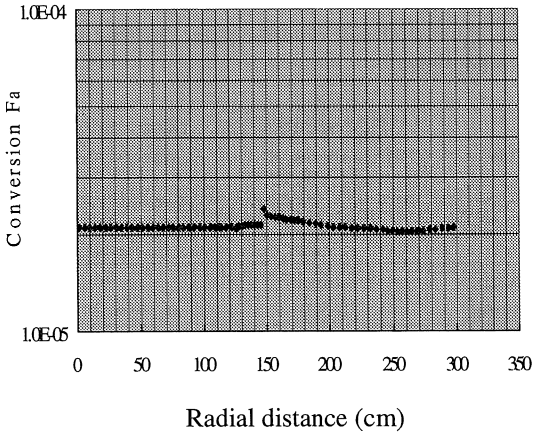

Fig. 7 Spatial distribution of the flux-to-dose conversion factor for the initial configuration in the radial (R) direction behind the primary closure plate in the unit of (μSv/h)/(n/cm2/s) for the cooling time of 10^6 seconds

Table 3 Summary of the Monte Carlo calculations for the equatorial maintenance port

		Initial configuration	Final configuration
Tally No.	Tally Location	Fast neutron flux (f.s.d.%)	Fast neutron flux (f.s.d.%)
1	within V.V. port (center)	2.47E+08 (4.8)	4.97E+08 (5.2)
2	above V.V port	1.68E+07 (10.3)	3.52E+07 (11.2)
3	behind 1st closure plate (center)	8.14E+06 (10.4)	5.92E+06 (28.6)
4	behind 1st closure plate (upper)	9.68E+06 (18.4)	7.11E+06 (16.7)
5	behind cryostat (center)	5.03E+06 (10.7)	4.18E+06 (20.7)
6	behind cryostat (upper)	4.52E+06 (9.4)	5.48E+06 (17.8)
7	behind cryostat (lower)	1.05E+07 (13.3)	8.01E+06 (30.6)

conversion factor for the initial configuration is shown in **Fig.6**, and the radial distribution (in the R direction) behind the primary closure plate is shown in **Fig.7**. In the space behind the primary closure plate (Z=1010 cm), the factor is almost constant, i.e. 2×10^{-5}.

2. Three-Dimensional Calculation

The results of the three-dimensional calculations are summarized in **Table 3**. The fast neutron flux behind the primary closure plate of the equatorial maintenance port is about 8.1×10^6 cm^{-2}s^{-1} (fractional standard deviation: 10%) for the initial configuration. It agrees well to the 2-D results described before (i.e. 8 to 10×10^6 cm^{-2}s^{-1}).

Table 4 Fast neutron flux and dose rate 10^6 s after shutdown around the equatorial and divertor ports (behind the primary closure plates)

Port	Fast neutron flux (n/cm^2 s) (f.s.d. %)	Dose rate (μSv/h) (Conversion Factor)
Equatorial	5.92E+06 (28.6)	89 (C. F.= 1.5E-5)
Divertor /pumping	4.70 E+06 (8.50)	94 (C. F.= 2.0E-5)
Divertor /maintenance	1.04 E+07 (8.73)	208 (C. F.= 2.0E-5)

The fast neutron flux is 5.9×10^6 cm^{-2}s^{-1} (fsd:29%) for the final configuration. It also agrees well to the 2-D results described before (i.e. 4 to 8×10^6 cm^{-2}s^{-1}), though the statistical error is rather large. The error is larger in the final configuration because the streaming neutrons through the gaps become more important in the final configuration due to the large gap widths and the thicker primary closure plate.

Applying the conversion factors to these neutron fluxes, the shutdown dose rates were estimated to be 162μSv/h and 89μSv/h for the initial and the final configurations, respectively. The latter case, the final configuration, may satisfy the design target of 100μSv/h.

The shutdown dose rates behind the closure plates of the equatorial maintenance port, divertor pumping ports and the divertor maintenance ports are summarized in **Table 4**, though the calculation process for the divertor ports are not described in this paper. The dose rate for the divertor maintenance ports is higher than 200μSv/h and exceeds the design target of 100μSv/h by a factor of two. The design target can be satisfied if the thickness of the closure plate increases from 20 cm to 30 cm.

IV. Conclusions

As a result of the analyses by the 2-D/3-D combined approach, it is found that the dose rate around the equatorial and divertor ports 10^6 seconds (11.6 days) after reactor shutdown ranges from 100 to 200μSv/h. The equatorial maintenance port and the divertor pumping port may satisfy the design target of 100μSv/h. The divertor maintenance ports, however, exceeds the design target by a factor of two and need shielding modification.

Another issue to be examined is uncertainty of the flux-to-dose conversion factor to be applied to the 3-D neutron flux. It is dependent upon the geometry as described above. It is necessary to use the proper factor generated with nearly the same geometry as the actual configuration.

Further, around the cooling water pipes, locally, gamma-rays from the radioactive corrosion products and from the materials activated by neutrons from ^{17}N in water (produced via ^{17}O(n,p) reaction) also contribute to the dose rate. The dose rate may exceed the design target locally. Therefore, attempts to further reduce the dose rate by improving the shield design, e.g. placing a shield block behind the gap, should be continued to follow the principle of ALARA (as low as reasonably achievable).

— References —

(1) "Technical Basis for the ITER Final Design Report, Cost Review and Safety Analysis (FDR)" (1998).

(2) Briesmeister, J. F., ed. : "MCNP-4B – A General Monte Carlo N-Particle Transport Code", *LA*-12625 *M* (1997).

(3) Rhoades, W. A., Mynatt, F. R. : "The DOT-III Two Dimensional Discrete Ordinates Transport Code", *ORNL-TM*-4280 (1973).

(4) Kosako, K., *et al.* : "Production and Verification of the MCNP cross section library FSXLIB-J3R2 based on JENDL-3.2", *Proc. 1996 Topical Meeting on Radiation Protection and Shielding*, **Vol.1**, p. 1088-1095 (1996).

(5) Maki, K., *et al.* : "Nuclear Group Constant Set FUSION-J3 for Fusion Reactor Nuclear Calculation Based on JENDL-3", *JAERI-M* 91-072 (1991).

(6) Seki, Y., *et al.* : "THIDA-2: An Advanced Code System for Calculation of Transmutation, Activation, Decay Heat and Dose rate", *JAERI-1301* (1986).

(7) Sato, S., *et al.* : "Evaluation of Biological Dose Rates around the ITER NBI Ports by 2-D S_N/Activation and 3-D Monte Carlo Analyses", to be published in *Fusion Engineering and Design*.

(8) *ITER Material Properties Handbook*, to be published.